American Journal of Pathology, Vol. 141, No. 5, November 1992
Copyright © American Association of Pathologists

Differential Permeability of the Blood–Brain Barrier in Experimental Brain Metastases Produced by Human Neoplasms Implanted into Nude Mice

Ruo-dan Zhang, Janet E. Price, Takamitsu Fujimaki, Corazon D. Bucana, and Isaiah J. Fidler

From the Department of Cell Biology, The University of Texas, M. D. Anderson Cancer Center, Houston, Texas

This study clarified whether and when the blood–brain barrier in experimental brain metastases is impaired by using hydrosoluble sodium fluorescein (MW 376) as a blood–brain barrier function indicator. Cells from eight human tumor lines (four melanomas, two breast carcinomas, one colon carcinoma, and one renal carcinoma) were inoculated into the internal carotid artery of nude mice. Brain metastases at different stages of development were sampled and the permeability of the blood–brain barrier around the metastases determined. Histologic examination showed two patterns of tumor growth. In the first, tumor cells formed isolated, well-defined nodules in the parenchyma of the brain. In lesions smaller than 0.2 mm^2, the blood–brain barrier was intact. In the second, small diffuse nests of tumor cells were distributed throughout the brain parenchyma. The blood–brain barrier was intact until the small tumor cell colonies coalesced to form large tumor masses. These results suggest that the permeability of the blood–brain barrier varies among different experimental brain metastases and that its function is related to the growth pattern and size of the lesions. (Am J Pathol 1992, 141:1115–1124)

The microvasculature of the brain parenchyma is lined by a continuous, nonfenestrated endothelium with tight junctions and little pinocytic vesicle activity.[1–4] This structure, designated as the blood–brain barrier, limits the entrance of circulating macromolecules into the brain parenchyma. The blood–brain barrier and the lack of a lymphatic system are responsible for maintaining the brain as an immunologically privileged site[5–7] and protecting the brain against the entry of most drugs and invasion by microorganisms.[8] The blood–brain barrier does not prevent the invasion of the brain parenchyma by circulating metastatic cells. Indeed, metastases in the brain develop in 10% to 40% of all patients with solid tumors.[9,10] The integrity of the blood–brain barrier is altered in some brain tumors and in metastases.[11–19] Added complexity is also presented by findings that some, but not all, neoplastic cells can affect the integrity of this structure.[12,13,20,21]

In general, primary brain neoplasms and brain metastases are resistant to treatment by most chemotherapeutic drugs,[6,8–10] and this resistance has been attributed to the inability of drugs to cross the blood–brain barrier.[22–25] Because this structure is morphologically, biochemically, and functionally heterogeneous in different regions of the brain,[1,4,26–28] its relationship to the failure to eradicate brain metastases with anticancer drugs is still unclear. The purpose of this study was to investigate the functional viability of the blood–brain barrier in brain metastases of different histologic origins. Because experimental studies of the integrity of the blood–brain barrier after direct injection of tumor cells into the brain of rodents have produced contradictory results[17,29–31] and direct injection can induce pathology, we have developed an experimental animal model to study the establishment, progression, and therapy of brain metastases.[31–33] Tumor cells are injected into the internal carotid artery of mice. Under the appropriate conditions, brain tumor lesions are produced in a reproducible manner, and the mice do not die of rapidly progressing visceral metastases.[32] Using this model, we have recently described the successful establishment of brain metastases of human melanomas and carcinomas in nude mice.[34,35] We have taken advantage of this ani-

Supported in part by Cancer Center Support Core grant CA 16672 and NIH grant R35-CA 42107 from the National Cancer Institute.

Accepted for publication May 8, 1992.

Address reprint requests to Dr. Isaiah J. Fidler, Department of Cell Biology (HMB 173), The University of Texas, M. D. Anderson Cancer Center, 1515 Holcombe Boulevard, Houston, TX 77030.

mal model for brain metastasis to examine the functional integrity of the blood–brain barrier in brain metastases of eight different human neoplasms growing in nude mice. Specifically, we wished to determine the status of the blood–brain barrier in early (small) and late (large) metastases growing in different regions of the brain. The results suggest that the blood–brain barrier is intact in the small lesions but permeable in metastases exceeding 0.2 mm^2.

Materials and Methods

Mice

Six- to eight-week-old, specific pathogen-free, athymic NCr-nu/nu mice were purchased from the Animal Production Area, NCI-Frederick Cancer Research Facility (Frederick, MD). Female mice were used for studying breast carcinoma cells, and male mice were used for studying other neoplasms. The mice were maintained in facilities approved by the American Association for Accreditation of Laboratory Animal Care and in accordance with current regulations and standards of the United States Department of Agriculture, Department of Health and Human Services, and National Institutes of Health.

Human Cancer Cell Lines

The human melanoma cell lines were originally isolated from metastases in different patients. The cell lines designated TXM were established from surgical specimens from melanoma patients at The University of Texas M. D. Anderson Cancer Center (Houston, TX): TXM-13, TXM-18, and TXM-34 were isolated from brain metastases. The A375 cell line, isolated originally from a lymph node metastasis, was injected intravenously into nude mice, and a variant designated A375-SM was isolated in culture from the resulting lung metastases.[35]

MDA-MB-435 and MDA-MB-468 are human breast carcinoma lines isolated originally from pleural effusions of two patients with advanced disease.[34] The two cell lines were the gift of Dr. Relda Cailleau, M. D. Anderson Cancer Center, Houston, TX.

The human colon cancer line $KM12L_4$ is a highly metastatic variant isolated by an *in vivo* selection procedure in nude mice from a surgical specimen of Dukes' stage B2 colon carcinoma.[36]

The human renal carcinoma cell line SN12A was derived from ascites produced in nude mice subsequent to intrakidney injection of cells isolated from a surgical specimen.[37]

In Vitro *Cultures*

The tumor cells were maintained as monolayer cultures on plastic in Eagle's minimum essential medium supplemented with 10% fetal bovine serum, sodium pyruvate, nonessential amino acids, L-glutamine, and twofold vitamin solution (GIBCO, Grand Island, NY). The cultures were incubated in 5% CO_2–95% air at 37°C. All cultures were free of Mycoplasma and the following murine viruses: reovirus type 3, pneumonia virus, Sendai virus, minute virus, mouse adenovirus, mouse hepatitis virus, and lactate dehydrogenase virus (assayed by M. A. Bioproducts, Walkersville, MD). For *in vivo* studies, tumor cells in their exponential growth phase were harvested by a 1-minute treatment with 0.25% trypsin-0.02% ethylenediaminetetra-acetic acid (EDTA) solution (wt/vol). The flask was tapped to detach the cells, supplemented medium was added, and the cell suspension was gently agitated to produce a single-cell suspension. The cells were washed and resuspended in Ca^{2+}-, Mg^{2+}-free Hanks' balanced salt solution (HBSS). Only suspensions of single cells with viability exceeding 90% were used (trypan blue exclusion test). The inoculum volume for injection into the internal carotid artery was 0.1 ml.

Injection of Cells into the Internal Carotid Artery

Each mouse was anesthetized by intraperitoneal injection of pentobarbital sodium, restrained on its back on a cork board, and placed under a dissecting microscope. The animal's head was stabilized on the cork board with a fixed rubber band placed between the teeth of the upper jaw. The neck was prepared for surgery with alcohol-iodine, and the skin was cut by a mediolateral incision. After blunt dissection, the trachea was exposed. The muscles were separated to expose the right common carotid artery, which then was separated from the vagal nerve. The artery was prepared for an injection distal to the point of division into the internal and external carotid arteries. A ligature of 5–0 silk suture was placed in the distal part of the common carotid artery, and a second ligature was placed and tied proximal to the injection site. The right carotid artery was nicked with a pair of microscissors, and a glass cannula was inserted into the lumen and threaded forward into the internal carotid artery. To assure proper delivery, we injected the cells slowly into the artery and then removed the cannula. The second ligature was tightened; the skin was closed by sutures. All intracarotid artery injections were always done under a dissecting microscope, and all required a glass cannula with a smaller than 30-gauge diameter. We prepared such cannulas from glass capillary tubes 1 mm in diam-

eter that were heated and then stretched, and each could be used repeatedly. The cannulas were fixed to 1-ml plastic syringes by melting the hub around them.

Histologic Examination of the Blood–Brain Barrier by Injection of Sodium Fluorescein and Use of the Freeze-dried Paraffin-embedded Tissue Technique

We injected 1×10^5 viable tumor cells into the internal carotid artery of nude mice (three to five per group). At different time points thereafter, we injected 0.5 mg of sodium fluorescein (mol wt, 376)/10 g body weight into a lateral tail vein, and the animals were killed 10 minutes later.[31] The brains were removed and processed for histologic examination by a freeze-dried paraffin-embedded tissue technique that preserves the distribution of the soluble fluorescent label.[38] Each brain was cut in four coronal sections of equal width to assure representative sampling and adequate comparison between the right and left hemispheres. Tissue was frozen in liquid nitrogen and stored at −70°C. After all the samples were collected, they were desiccated in a lyophilizer for 7 days at −50C. Thereafter, the brains were embedded in paraffin, and serial 6-μ tissue sections were cut. The function of the blood–brain barrier was determined immediately after carotid artery injection and at 10 minutes, 1 hour, 2 hours, 4 hours, 7 hours, 24 hours, 3 days, 7 days, 10 days, 14 days, 21 days, 28 days, 42 days, and 56 days after inoculation of tumor cells. For each tumor, we examined at least 50 sections. Every other section was stained with hematoxylin and eosin. From these sections, we selected those containing the largest diameter tumor nodules. The area of each nodule was measured by image analysis in an IBAS Image Analyzer (Carl Zeiss, Inc., Thornwood, NY).

Results

Validation of the Injection Procedure

The first experiment was designed to rule out the possibility that the injection of tumor cells into the carotid artery and the introduction of a bolus of tumor cells into the brain, followed by the ligation of the injected artery, could damage and compromise the blood–brain barrier. Mice were given intracarotid injections of 0.1 ml HBSS or 1×10^5 viable $KM12L_4$ colon carcinoma cells suspended in 0.1 ml HBSS. The viability of the blood–brain barrier was determined immediately after the intracarotid injection and at various intervals thereafter (10 minutes, 20 minutes, 30 minutes, 1 hour, 2 hours, 4 hours, 6 hours, 8 hours, 12 hours, 24 hours, 2 days, 3 days, 4 days, and 7 days). At each of the time points, we studied the pattern of sodium fluorescein distribution in the brains of three mice. At all of these time points, the blood–brain barrier was intact (Figure 1). The lumina of the vessels were small, and the sodium fluorescein tracer was confined to the vessels. The meninges were fluorescent. The distribution of sodium fluorescein in the right and left hemispheres was similar despite the ligation of the right carotid artery, indicating that the procedure of inoculating tumor cells into the brain blood circulation did not compromise the function of the blood–brain barrier. The injection of tumor cells into the right carotid artery produced experimental brain metastases in the right hemisphere. When the lesions were larger than 0.5 mm in diameter, some tumor cells invaded the left hemisphere and ventricle. Carcinomatous meningitis was not observed.

The Blood–Brain Barrier in Early Stages of Experimental Brain Metastases

Experimental brain metastases are established from the proliferation of few surviving cells.[33–35] The histologic identification of a tumor colony (metastases) in the brain can be accomplished when the cut section of a lesion shows a cluster of 10 or more tumor cells (Figure 2A). This size lesion was found 7 to 25 days after intracarotid injection of different human tumor cells. Regardless of the injected tumor cells, no leakage of sodium fluorescein was found in and around the emerging, experimental brain metastases, indicating that the blood–brain barrier was intact. The data using the human colon cancer cell line $KM12L_4$ 10 days after inoculation into the carotid artery are shown in Figure 2A and B. The tumor lesions appeared avascular. The morphology of the blood vessels near the small developing metastases did not differ from that observed in the brain tissue of the opposite, unaffected hemisphere.

Permeability of the Blood–Brain Barrier in Brain Metastases of Different Sizes Produced by Different Human Neoplasms

We have previously shown that the pattern of brain metastases and their growth rate varies among different neoplasms.[31–35] In this study, we injected nude mice with cells of eight different human tumors. The different neoplasms could be divided into two major groups according to their growth pattern in the brain. The first group, consisting of MDA-MB-435 and MDA-MB-468 breast carcinoma, $KM12L_4$ colon carcinoma, SN12A renal cell cancer, and TXM-34 and A375-SM melanomas, was

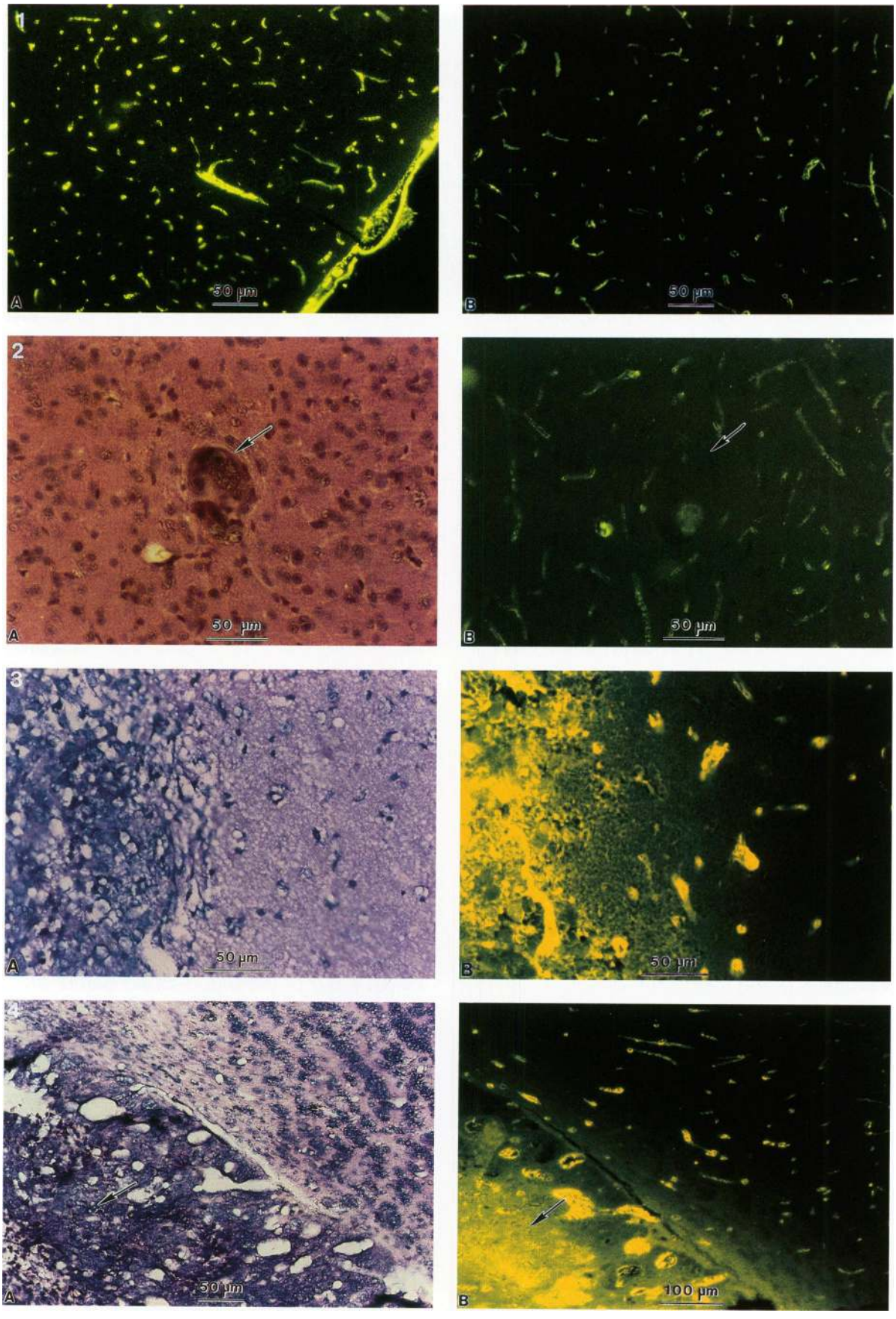
1
A
50 μm
B
50 μm
2
A
50 μm
B
50 μm
3
A
50 μm
B
50 μm
4
A
50 μm
B
100 μm

Figure 1. *Intravenous injection of sodium fluorescein into* (A) *normal mice and* (B) *mice previously given injections of KM12L$_4$ colon carcinoma into the internal carotid artery 7 days before analysis showed intact blood-brain barrier. Sodium fluorescein was found exclusively inside blood vessels and the meninges, ×250.*
Figure 2. *A small brain tumor* (A, *arrow*) *10 days after intracarotid artery injection of KM12L$_4$ showed no leakage of sodium fluorescein in its immediate vicinity* (B). *The label was observed only inside the blood vessels. The location of the tumor is indicated by an arrow in the fluorescence micrograph* (B), *×344.*
Figure 3. *Experimental brain metastases (0.78 mm^2) 4 weeks after intracarotid artery injection of SN12A renal cell carcinoma showed extensive leakage of the sodium fluorescein in and surrounding the tumor.* A, *H&E stain;* B, *fluorescence. ×370.*
Figure 4. *A large brain metastasis (3 mm^2) 4 weeks after intracarotid artery injection of KM12L$_4$ colon carcinoma cells showed central necrosis* (A, *arrow*). *Fluorescence microscopy of this area showed diffuse fluorescence only in the necrotic area* (B, *arrow*). *At the periphery of the tumor, fluorescence was seen only inside blood vessels, ×172.*

characterized by the formation of multifocal, circumscribed lesions in the brain parenchyma. The second group of tumors, consisting of melanoma cell lines TXM-13 and TXM-18, was characterized by the formation of multiple diffuse tumor cell clusters (see below).

The size of individual brain lesions increased with time. Representative data for lesions produced by KM12L$_4$ colon carcinoma cells are shown in Table 1. The leakage of fluorescein in and around brain metastases was directly correlated with the size of individual lesions and not with their location in the brain parenchyma. We base this conclusion on the following data: In nude mice given injections of different human neoplasms, leakage of fluorescein was only found in lesions exceeding 0.2 mm^2 (0.5 mm in diameter) (Figure 3). We examined a large number of histologic sections of brains from nude mice given carotid artery injections of cells of different human neoplasms. Regardless of the tumor type or the location of the lesion in the nude mouse brain parenchyma, the blood–brain barrier was intact in lesions smaller than 0.2 mm^2 (Table 2).

With increasing size of individual experimental brain metastases, the number of irregular blood vessels within and surrounding the lesions increased. In most (> 70%) tumor lesions exceeding 0.5 mm in diameter, we observed some degeneration or necrosis. Intravenous injection of sodium fluorescein revealed that the blood–brain barrier in these lesions was not intact because leakage of the dye was often observed. An example of these findings is shown in Figure 3 with brain metastases of human renal cell carcinoma SN12A. Central necrosis of the lesion, however, was not necessarily associated with permeability of the vasculature. In many metastases with central necrotic zones, the periphery consisted of viable tumor tissue in which no leakage of fluorescein was found (Figure 4).

Table 1. *Size of Brain Metastases Produced by Human Colon Carcinoma KM12L$_4$ Cells Injected into the Carotid Artery of Nude Mice*

Time (weeks)	Number of lesions	Size (mm^2)	
		Median	Range
1	3	0.016	0.003–0.03
2	5	0.09	0.009–0.2
3	21	0.5	0.004–2.4
4	12	1.7	0.02–5.7
5	13	4.5	0.03–6.7

1 × 10^5 KM12L$_4$ cells were injected into the internal carotid artery of nude mice. Three mice were killed at the indicated times. The data are median size in mm^2 of experimental brain-parenchyma metastases.

Further evidence to support the conclusion that vascular leakage around brain metastases is correlated with their size is presented in Figure 5. In brain sections containing many KM12L$_4$ colon carcinoma metastases, leakage of fluorescein was found in lesions exceeding 0.2 mm^2. At the same time, no leakage of the dye was found in or around smaller lesions. Leakiness of sodium fluorescein was found in all tumors growing in the choroid plexus, regardless of size. This may be due to the fenestrated nature of blood vessels in the choroid plexus.[1,31]

Two human melanoma cell lines (TXM-13 and TXM-18) produced diffuse small clusters of tumor cells throughout the brain parenchyma without a defined margin (Figure 6). The morphology of the blood vessels (in and around the lesions) was not remarkable. Some of the vessels were enlarged but the blood–brain barrier was intact (Figure 6). The relationship of tumor size to the blood–brain barrier as described above for well-defined solitary metastases did not apply to the diffuse tumor lesions. Leakage of fluorescein was noted, however, when small tumor foci enlarged and coalesced to form tumor masses exceeding 2 mm in diameter and was associated with central necrosis.

Discussion

Results of previous studies on the permeability of the blood–brain barrier in neoplasms of the brain (primary and metastases) were contradictory. Many studies concluded that the blood–brain barrier is not intact in most brain lesions,[10,12,18,19,29] with the degree of blood–brain barrier permeability differing among different anatomic locations (in the brain) and the size of the lesions.[29,39] In other tumor systems, the blood–brain barrier was intact in and around experimental brain metastases.[31,40] The discrepancy in these results is likely due to observations with different tumors used under different experimental systems.[40] Clearly, even the same tumor cells could pro-

Table 2. *Size of Experimental Brain Metastases and Permeability of the Blood-brain Barrier to Sodium Fluorescein*

Tumor	Status of the blood-brain barrier	Size (mm^2)	
		Median	Range
A375-SM melanoma	Intact	0.004	0.003–0.006
	Permeable	3.7	1.6–9.1
TXM-34 melanoma	Intact	0.2	0.08–0.2
	Permeable	1.7	0.3–10.1
$KM12L_4$ colon carcinoma	Intact	0.06	0.003–0.2
	Permeable	1.2	0.3–16.7
SN12 renal carcinoma	Intact	0.2	0.02–0.2
	Permeable	0.8	0.3–3.9
MDA-435 breast carcinoma	Intact	0.1	0.01–0.2
	Permeable	0.5	0.3–0.9
MDA-468 breast carcinoma	Intact	0.01	0.007–0.1
	Permeable	4.3	0.3–6.5

1×10^5 viable tumor cells were injected into the internal carotid artery of nude mice. The mice were killed at different intervals thereafter (n = 3). The data are median size in mm^2 of at least 20 lesions/tumor line. Permeability of the blood-brain barrier was determined by vascular retention of sodium fluorescein.

duce different results subsequent to direct (intracerebral) injection or intracarotid inoculation.[29]

In the current study, we investigated eight different human tumor cell lines inoculated into the internal carotid arteries of nude mice. The tumors produced lesions in different regions of the brain, and the pattern of the lesions varied from diffuse to solitary with well-defined margins. The results demonstrate that the permeability of the blood–brain barrier in and around experimental brain metastases correlated with their size and, hence, with their pattern of growth.

Of several molecular tracers used to study the permeability of the blood–brain barrier, we chose sodium fluorescein.[37] Despite its low molecular weight (MW 376), this hydrosoluble molecule is excluded from the brain by an intact blood–brain barrier.[31,38,41,42] Sodium fluorescein is not sensitive to minor or transient changes in blood–brain barrier permeability, and unlike horseradish peroxidase, it is not transported into brain tissue by nonspecific endocytosis.[43] This molecule is therefore most suitable for studies of blood–brain barrier functions in brain metastases.

We have established an animal model to study the pathogenesis and therapy of experimental brain metastases that are established subsequent to inoculation of tumor cells into the internal carotid artery.[32–34,44,45] Before studying the function of the blood–brain barrier in such brain lesions, we had to rule out that the procedure of intracarotid injection, which is followed by ligation of the artery, or the entry of a bolus of tumor cells into the brain, may damage the endothelial cells of the cerebromicrovessels and, thus, change the permeability of the blood–brain barrier. We therefore examined the blood–brain barrier in a large number of mice that were killed at different times after the intracarotid injection of either HBSS or $KM12L_4$ cells. At no time (0 to 7 days postinjection) did we observe alterations in permeability of the blood–brain barrier. This finding validated the model for examining the blood–brain barrier in brain tumor lesions.

Previous data from our laboratory showed that mouse blood monocytes-macrophages infiltrate brain metastases produced by a fibrosarcoma growing in syngeneic immunocompetent mice, whereas activated T-lymphocytes were not detected.[31] This is in contrast to autoimmune encephalitis, where infiltration by T-lymphocytes is followed by macrophages.[38] These data therefore suggest that the absence of T-lymphocytes in nude mice does not present an artifact of this metastatic cascade.

The use of ^{14}C-labeled alpha-aminoisobutyric acid as a tracer demonstrated an increase in capillary permeability with increasing size of experimental brain metastases in rats.[29] Similarly, an increased blood–brain barrier permeability was found in brain tumors induced in rats.[19,30,46] Most of the evidence that human tumor cells can also induce such changes have been based on morphologic and not on functional observations.[12,15,16] Our observations of blood–brain barrier function in solitary brain metastases produced by different human tumor cells are in agreement with the previous studies in rats.[19,29,30,46] In rat tumors, however, the critical size of lesions that maintained an intact blood–brain barrier was 1 to 4 mm in diameter. In our study, the critical size of lesions with an intact blood–brain barrier was <0.2 mm^2 or 0.5 mm in diameter. Although these differences could be due to the use of different tracers, the possibility that the differences are also due to the origin of the tumors (human versus rat) cannot be excluded.

Leakage through the blood–brain barrier may be due to endothelial alterations brought about by tumor cells in the perivascular space.[47] Several ultrastructural studies concluded that brain tumors disrupt adjacent endothelium.[12,48] In our study with eight different human tumor cell lines, the lesions in the brain parenchyma were either

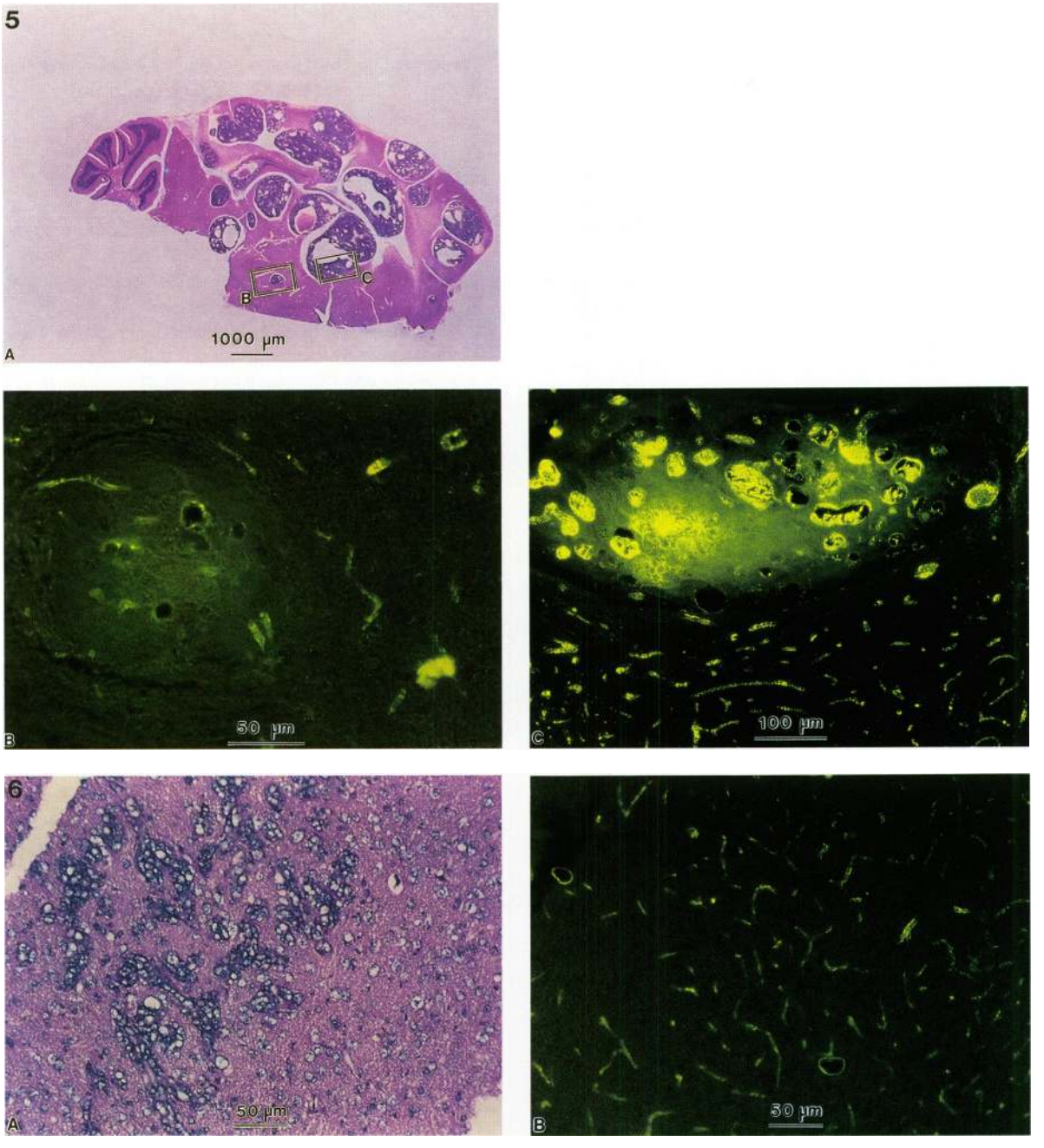

Figure 5. *Multiple brain parenchymal metastases of varying sizes 4 weeks after intracarotid artery injection of KM12L$_4$ colon carcinoma are shown in an H&E-stained section* (A). *The fluorescence of selected areas representing* (B) *small (<0.2 mm^2) and* (C) *large (>4.0 mm^2) tumor nodules showed diffuse fluorescence only in the large tumor nodule. Fluorescence was limited to the blood vessels in the brain parenchyma surrounding the tumor nodules, ×172.*

Figure 6. *The human melanoma TXM-13 injected into the carotid artery 50 days earlier exhibited a diffuse pattern of growth in the brain parenchyma* (A, *H&E stain). Fluorescence microscopy of the same area showed that sodium fluorescein was limited to the blood vessels only* (B), *×260.*

well demarcated with well-defined margins or diffuse lesions throughout a region of the parenchyma. We found that the solitary well-defined lesions had a lower density of blood vessels than normal brain tissue. The blood–brain barrier is known to become permeable in ischemic regions of the brain where increased endothelial pinocytosis, opening of the interendothelial tight junctions, and damage to endothelial cells have all been observed.[49] We found that degeneration and central necrosis often occurred in large (>0.5 mm in diameter, 0.2 mm^2) brain

metastases. In these lesions, therefore, damage to endothelial cells may compromise the integrity of the blood–brain barrier.

We have previously reported that the blood–brain barrier was intact in established mouse UV-2237 fibrosarcoma brain metastases.[31] Two human melanoma cell lines (TXM-13, TXM-18) studied here produced the same phenomenon. The common characteristic to these mouse and human brain metastases was their diffuse pattern of growth. The permeability of the blood–brain barrier in these lesions was not increased as compared with normal brain tissue unless the tumor cell clusters coalesced to form large tumor masses. Studies using the transplantation of quail avascularized embryonic mesodermal tissue into the brain of chick embryos[50] and an *in vitro* study of endothelial cell–astrocyte interactions[51] demonstrated that signals arising within the brain, rather than a programmed commitment of the endothelial cells, are responsible for the function of the blood–brain barrier. The integrity of the barrier around small lesions (metastases) shows that the barrier can repair after passage of metastatic cells into the brain parenchyma. Moreover, the interaction of astrocytes with endothelial cells and elongated cytoplasmic processes of oligodendrocytes are likely to be important in maintaining a functional blood–brain barrier.[1] A growing tumor mass may disturb this interaction, especially if it depends on contact between astrocytes and endothelial cells. In any event, the normal brain tissue interspersed among the small tumor clusters or surrounding small tumor lesions might be responsible for the normal function of the blood–brain barrier.

Clinical observations have concluded that primary brain cancers and brain metastases are relatively resistant to most chemotherapeutic drugs.[6–10] Experimental data with human tumor cells growing in the brain of nude mice support this conclusion.[52] Because the blood–brain barrier is not intact in experimental brain metastases that exceed 0.2 mm^2, the resistance to chemotherapy may be due to other mechanisms. We did not investigate whether the blood–brain barrier in experimental brain metastases is metabolically dysfunctional in glucose transport[53] or saturable molecules.[54] Future work should address this possibility.

In conclusion, the results indicate that the permeability of the blood–brain barrier in experimental brain metastases produced by eight different human tumor cells after injection into the carotid artery of nude mice was determined by the location of tumor lesions in the brain and by the size and pattern of growth of the lesions. These results may provide a useful reference for studies designed to understand the biology and therapy of brain metastases.

Acknowledgment

The authors thank Mr. Ricardo Sanchez for excellent technical assistance in the preparation of histologic specimens.

References

1. Tomlinson E: Theory and practice of site-specific drug delivery. Adv Drug Del Rev 1987, 1:187–198
2. Johansson BB: The physiology of the blood-brain barrier. Adv Exp Med Biol 1990, 274:25–39
3. Gregoire N: The blood-brain barrier. J Neuroradiol 1989, 16(3):238–250
4. Pardridge WM, Oldendorf WH, Cancilla P, Frank HJ: Blood-brain barrier: Interface between internal medicine and the brain clinical conference. Ann Intern Med 1986, 105(1):82–95
5. Medawar PB: Immunity to homologous grafted skin: III. The fate of skin homografts transplanted to the brain, to subcutaneous tissue, and to the anterior chamber of the eye. Br J Exp Pathol 1948, 29:58–69
6. Scheinberg LC, Edelman FL, Levy WA: Is the brain "an immunologically privileged site"? Arch Neurol 1964, 11:248–264
7. Felgenhauer K: The blood-brain barrier redefined. J Neurol 1986, 233:193–194
8. Shapiro WR, Shapiro JR: Principles of brain tumor chemotherapy. Semin Oncol 1986, 13:56–69
9. Kornblith PL, Walker MD, Cassady JR: Treatment of metastatic cancer to the brain, Cancer, Principles, and Practice of Oncology, 2nd edition, Vol 2. Edited by VT DeVita, S Hellman, SA Rosenberg. Philadelphia, JB Lippincott, 1985, pp 2099–2103
10. Zuelch KG: Brain tumors: Their biology and pathology, 3rd edition. Berlin, Springer-Verlag, 1986, pp 490–498
11. Debbage PL, Gabius HJ, Bise K, Marguth F: Cellular glycoconjugates and their potential endogenous receptors in the cerebral microvasculature of man: A glycohistochemical study. Eur J Cell Biol 1988, 46(3):425–434
12. Stewart PA, Hayakawa K, Farrell CL, Del Maestro RF: Quantitative study of microvessel ultrastructure in human peritumoral brain tissue. Evidence for a blood-brain barrier defect. J Neurosurg 1987, 67(5):697–705
13. Zagzag D, Goldenberg M, Brem S: Angiogenesis and blood-brain barrier breakdown modulate CT contrast enhancement: An experimental study in a rabbit brain-tumor model. AJR 1989, 153(1):141–146
14. Iannotti F, Fieschi C, ALfano B, Picozzi P, Mansi L, Pozzilli C, Punzo A, Del Vecchio G, Lenzi GL, Salvatore M: Simplified, noninvasive PET measurement of blood-brain barrier permeability. J Comput Assist Tomogr 1987, 11(3):390-197
15. Front D, Israel O, Kohn S, Nir I: The blood-tissue barrier of human brain tumors: Correlation of scintigraphic and ultrastructural findings (concise communication). J Nucl Med 1984, 25(4):461–465

16. Kohn S, Front D, Nir I: Blood-brain barrier permeability of human gliomas as determined by quantitation of cytoplasmic vesicles of the capillary endothelium and scintigraphic findings. Cancer Invest 1989, 7(4):313–321
17. Nir I, Levanon D, Iosilevsky G: Permeability of blood vessels in experimental gliomas: Uptake of ^{99}Tc-glucoheptonate and alteration in blood-brain barrier as determined by cytochemistry and electron microscopy. Neurosurgery 1989, 25(4):523–532
18. Coomber BL, Stewart PA, Hayakawa K, Farrell CL, Del Maestro RF: Quantitative morphology of human glioblastoma multiform microvessels: Structural basis of blood-brain barrier defect. J Neurooncol 1987, 5(4):299–307
19. Vriesendorp FJ, Peagram C, Bigner DD, Groothuis DR: Concurrent measurements of blood flow and transcapillary transport in xenotransplanted human gliomas in immunosuppressed rats. J Natl Cancer Inst 1987, 79(1):123–130
20. Nicolson GL: Organ specificity of cancer metastasis is determined, in part, by tumor cell properties and cytokines expressed at particular organ sites. Am Assoc Cancer Res 1990, 31:506–507
21. Schlingemann RO, Rietveld FJ, De Wall RM, Ferrone S: Expression of the high molecular weight melanoma-associated antigen by pericytes during angiogenesis in tumors and in healing wounds. Am J Pathol 1990, 136(6): 1393–1405
22. Greig NH: Optimizing drug delivery to brain tumors. Cancer Treat Rev 1987, 13(1):1–28
23. Genka S, Deutsch J, Stahle PL, Shetty UH, John V, Robinson C, Rapoport SI, Greig NH: Brain and plasma pharmacokinetics and anticancer activities of cyclophosphamide and phosphoamide mustard in the rat. Cancer Chemother Pharmacol 1990, 27(1):1–7
24. Greig NH, Soncrant TT, Shetty HU, Momma S, Smith QR, Rapoport SI: Brain uptake and anticancer activities of vincristine and vinblastine are restricted by their low cerebrovascular permeability and binding to plasma constituents in rat. Cancer Chemother Pharmacol 1990, 26(4):263–268
25. Freeman AI, Fenstermacher J, Shapiro W, and 28 additional authors: Forbeck forum on improved drug delivery to brain tumors. Sel Cancer Ther 1990, 6(3):109–118
26. Owman C, Hardebo JE: Functional heterogeneity of the cerebrovascular endothelium. Brain Behav Evol 1988, 32(2): 65–75
27. Fenstermacher J, Gross P, Sposito N, Acuff V, Pettersen S, Gruber K: Structural and functional variations in capillary systems within the brain. Ann NY Acad Sci 1988, 529:21–30
28. Baur HC, Tontsch U, Amberger A, Bauer H: Gamma-glutamyl-transpeptidase (GGTP) and NA+K(+)-ATPase activities in different subpopulations of cloned cerebral endothelial cells: Responses to glial stimulation. Biochem Biophys Res Commun 1990, 168(1):358–363
29. Hasegawa H, Ushio Y, Hayakawa T, Yamada K, Mogami H: Changes of the blood-brain barrier in experimental metastatic brain tumors. J Neurosurg 1983, 59:304–310
30. Shapiro WR, Hiesiger EM, Cooney GA, Basler GA, Lipschutz LE, Posner JP: Temporal effects of dexamethasone on blood-to-brain and blood-to-tumor transport of ^{14}C-alpha-aminoisobutyric acid in rat C6 glioma. J Neurooncol 1990, 8(3):997–1204
31. Schackert G, Simmons RD, Buzbee TM, Hume DA, Fidler IJ: Macrophage infiltration into experimental brain metastases: Occurrence through an intact blood-brain barrier. J Natl Cancer Inst 1988, 80(13):1027–1034
32. Schackert G, Fidler IJ: Development of *in vivo* models for studies of brain metastasis. Int J Cancer 1988, 41(4):589–594
33. Schackert G, Fidler IJ: Site-specific metastasis of mouse melanomas and a fibrosarcoma in the brain or meninges of syngeneic animals. Cancer Res 1988, 48(12):3478–3484
34. Schackert G, Price JE, Bucana DC, Fidler IJ: Unique patterns of brain metastasis produced by different human carcinomas in athymic nude mice. Int J Cancer 1989, 44(5): 892–897
35. Schackert G, Price JE, Zhang RD, Bucana CD, Itoh K, Fidler IJ: Regional growth of different human melanomas as metastases in the brain of nude mice. Am J Pathol 1990, 136(1):95–102
36. Morikawa K, Walker SM, Jessup JM, Fidler IJ: *In vivo* selection of highly metastatic cells from surgical specimens of different primary human colon carcinomas implanted into nude mice. Cancer Res 1988, 48:1943–1948
37. Naito S, von Eschenbach AC, Giavazzi R, Fidler IJ: Growth and metastasis of tumor cells isolated from a human renal cell carcinoma implanted into different organs of nude mice. Cancer Res 1986, 46:4109–4115
38. Simmons RD, Buzbee TM, Linthicum DS, Mandy WJ, Chen G, Wang C: Simultaneous visualization of vascular permeability change and leukocyte egress in the central nervous system during autoimmune encephalomyelitis. Acta Neuropathol 1987, 74(2):191–193
39. Bradbury MW, Lightman SL: The blood-brain interface. Eye 1990, 4:249–254
40. Terada T, Nishiguchi T, Hyoutani G, Miyamoto K, Nakamura Y, Tsuura M, Komai N: A study on the vascular permeability of brain tumors using dynamic CT. No Shinkei Geka 1989, 17(9):841–848
41. Nakagawa Y, Fujimoto N, Matsumoto K, Cervos Navarro J: Morphological changes in acute cerebral ischemia after occlusion and reperfusion in the rat. Adv Neurol 1990, 52:21–27
42. Kawamura S, Schurer L, Goetz A, Kempski O, Schmucker B, Baethmann A: An improved closed cranial window technique for investigation of blood-brain barrier function and cerebral vasomotor control in the rat. Int J Microcirc Clin Exp 1990, 9(4):369–383
43. Malmgren LT, Olsson Y: Differences between the peripheral and the central nervous system in permeability to sodium fluoresein. J Comp Neurol 1980, 191:103–117
44. Schackert G, Fan D, Nayar R, Fidler IJ: Arrest and retention of multilamellar liposomes in the brain of normal mice or mice bearing experimental brain metastases. Sel Cancer Ther 1989, 5(2):73–79

45. Zhang RD, Price JE, Schackert G, Itoh K, Fidler IJ: Malignant potential of cells isolated from lymph node or brain metastases of melanoma patients and implications for prognosis. Cancer Res 1991, 51(8):2029–2035
46. Yamada K, Ushio Y, Hayakawa T, Kato A, Yamada N, Mogami H: Quantitative autoradiographic measurements of blood-brain barrier permeability in the rat glioma model. J Neurosurg 1982, 57:394–398
47. Ballinger WE Jr, Schimpff RD: An experimental model for cerebral metastases: Preliminary light and ultrastructural studies. J Neuropath Exp Neurol 1979, 38:19–34
48. Hirano A, Zimmerman HM: Fenestrated blood vessels in a metastatic renal carcinoma in the brain. Lab Invest 1972, 26:465–468
49. Dietrich WD, Busto R, Halley M, Valdes I: The importance of brain temperature in alterations of the blood-brain barrier following cerebral ischemia. J Neuropathol Exp Naurol 1990, 49(5):486–497
50. Stewart PA, Wiley MJ: Development of nervous tissue induces formation of blood-brain barrier characteristics in invading endothelial cells: A study using quail-chick transplantation chimeras. Dev Biol 1981, 84:183–192
51. Goldstein GW: Endothelial cell-astrocyte interactions: A cellular model of the blood-brain barrier. Ann NY Acad Sci 1988, 529:31–39
52. Fidler IJ, Schackert G, Zhang RD, Price JE: Experimental models to study melanoma brain metastasis. Proceedings, International Conference on Biological Treatment of Melanoma and Other Cancers. Edited by P Hersey. University of Newcastle Press, Australia, 1990, pp 210–220
53. Harik SI, Roessmann U: The erythrocyte-type glucose transporter in blood vessels of primary and metastatic brain tumors. Ann Neurol 1991, 29:5
54. Banks WA, Kastin AJ: Aluminum-induced neurotoxicity: Alterations in membrane function at the blood-brain barrier. Neurosci Biobehav Rev 1989, 13(1):47–53